Available online at www.sciencedirect.com

ScienceDirect

Procedia CIRP 123 (2024) 179–184

www.elsevier.com/locate/procedia

7th CIRP Conference on Surface Integrity

Investigation of the surface topography and cutting tool kinematics in Hammering Turning

Jannik Schwalm[a,*], Mike Görtz[b], German Gonzalez[a], Volker Schulze[a], Frederik Zanger[a]

[a]*wbk Institute of Production Science, Karlsruhe Institute of Technology (KIT), Kaiserstr. 12, 76131 Karlsruhe, Germany*
[b]*Faculty of Mechanical Engineering, Karlsruhe Institute of Technology (KIT), Kaiserstr. 12, 76131 Karlsruhe, Germany*

* Corresponding author. Tel.: +49-721-608-42455; fax: +49-721-608-45004. *E-mail address:* jannik.schwalm@kit.edu

Abstract

Hammering Turning is a new process combination of Vibratory Assisted Machining (VAM), which can achieve both microtexturing of the surface and hardening through mechanical surface treatment by suitable coupling of a biaxial oscillation of the cutting tool. These surfaces can be used for optimising tribological applications. Microtextures are formed by plastic deformation of the surface layer which is decoupled from the cutting process. The excitation of the oscillation is done by an open loop piezo system. In this work, a correlation of microtextured topographies and process forces with measured displacement signals using a non-contact capacitive measurement system with submicrometer resolution is presented. Further, the influence of different tool microgeometries on the process forces, kinematics of the process and the resulting topography is investigated. The results show that especially the tool geometry has a large influence on the type of microtexture, while process forces are affected to a minimum.

Keywords: Texture; Surface analysis, Piezoelectric

1. Introduction

This study deals with Vibratory Assisted Machining (VAM). In this process, an actuator system is used to induce a low-amplitude vibration in either the cutting tool or the workpiece. The beginnings of this technology date back to the late 1950s, when the first experiments with one-dimensional vibration were carried out [1]. One of the earliest publications describes the application of an electrohydraulic actuator system for vibration-assisted longitudinal turning that used one-dimensional sinusoidal vibration. This achieved vibration frequencies of up to *125 Hz* and a constant vibration amplitude of *101.6 μm* [2].

In current research, various forms of vibration-assisted machining are differentiated. These include one-, two-, and three-dimensional vibration assistance, as well as resonant and non-resonant vibration systems [3]. On the one hand resonant systems can achieve frequencies up to the ultrasonic band at amplitudes of about *10 μm* [4–7]. Non-resonant systems, on the other hand, do not achieve such high frequencies, but offer greater flexibility in terms of their kinematics, as they do not rely on the superposition of harmonic vibrations. This allows adjustment of vibration frequency, amplitude, and excitation function freely without being limited to sinusoidal mode [3].

Actuators used today in vibration-assisted machining are mainly piezoelectric and electromagnetic actuators due to their high dynamic performance [3, 8]. Occasionally, other actuator principles such as hydraulic actuators are also used [9]. Furthermore, these processes can be divided into two categories depending on the purpose of the vibration: Processes in which vibration is used to improve the machining process and processes in which vibration is used to texture the surface of the workpiece.

In the context of combining vibration-assisted machining and machine surface hammering, the combination process of Hammering Turning was developed [10]. Here, two

2212-8271 © 2024 The Authors. Published by Elsevier B.V.

10.1016/j.procir.2024.05.033

piezoelectric actuators in the non-resonant band of vibration frequencies are used to achieve mechanical surface treatment and microtexturing simultaneously with machining. The orthogonal configuration of the piezoelectric actuators allows a synchronized kinematic that decouples the hammering movement from the cutting process. This can enable the generation of deeper residual compressive stresses in the near-surface layer of the workpiece compared to conventional vibration-assisted machining [11]. For decoupling, one of the actuators generates a sinusoidal tool motion in the cutting direction, resulting in the superposition of this motion with the cutting speed. The effective relative speed between workpiece and tool during the hammering motion is close to zero. In this paper, microtextured topographies resulting from Hammering Turning as well as process forces and measured displacement signals from the process are presented. Furthermore, the influence of different tool microgeometries on process forces, process kinematics and the resulting topography is investigated. This is the basis for an inverse approach to identify parameters for a controlled microtexturing with Hammering Turning. The aim of the Hammering Turning is a microtexturing of the surface which is suitable for the adjustment of the tribological properties. For this purpose, the influencing process parameters and their influences must be investigated.

2. Experimental Setup

Since in Hammering Turning the resulting topography of the surface is caused by plastic deformation of the surface layer by the cutting tool, the microgeometry of the cutting edge is crucial. For the experiments, the cutting edges of cutting inserts were prepared by brushing to achieve a defined microgeometry. In addition to the microgeometry, the control of displacement of the tool is essential for Hammering Turning. For this purpose, a non-contact capacitive measuring system was integrated into the piezo tooling system.

2.1. Process parameters

The experiments were carried out on an Index V100 vertical turning machine. The piezo tool system for Hammering Turning, as described in Figure 1, was integrated on this machine. In addition to the tool microgeometry, the investigation focused on the influence of the feed rate, while other process parameters such as cutting speed were kept constant, see Table 1. Samples of AISI4140 steel (42CrMo4) quenched and tempered at *450 °C* with a diameter of *20 mm* were used. For each parameter set, the sample was machined to a length of *2 mm* in z-direction. To minimize clamping errors such as runout and positional errors, all samples were machined in the same clamping with the same tool as in the experiment, with a feed rate of *0.05 mm/rev* and the same cutting speed (*0.5 m/min*) and cutting depth (*0.1 mm*).

Table 1. Process parameters Hammering Turning.

Process parameter	Value
Feed rate f_c [mm/rev]	0.05; 0.06; 0.07; 0.08; 0.09; 0.1
Cutting speed v_c [m/min]	0.5
Hammer frequency f_H [Hz]	133
Depth of cut a_p [mm]	0.1

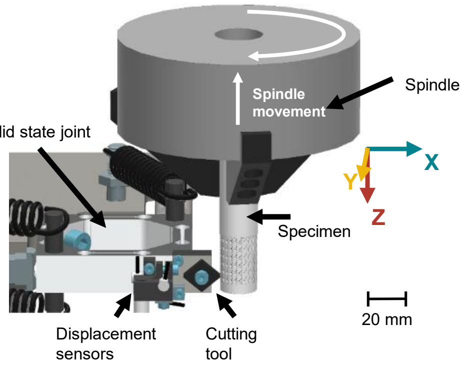

Figure 1: Experimental setup for Hammering Turning.

2.2. Tool preparation

For the investigation, uncoated carbide inserts of the substrate HTi10 from Mitsubishi Materials with the ISO geometry CCMW120404 from were used. For the experiments, these were used in the unprepared condition and with a custom prepared cutting edge. The cutting edges were prepared by brushing with a round brush made of *0.3 mm* nylon bristles with embedded SiC grains, the grit size was F320, which corresponds to a grain size of *30 µm*. Since brushing was intended to achieve a greater rounding of the cutting edge, the brushing direction was set from the rake face to the flank, with the rake face perpendicular to the axis of rotation. Further parameters can be found in Table 2. The microgeometry of the cutting edge was characterized according to Denkena [12]. Table 3 shows the initial condition of the microgeometry as well as the prepared condition and also the values of the unprepared insert in the experiments.

Table 2. Process parameters brushing.

Parameter	value
Diameter [mm]	50
Rotational speed [min^{-1}]	1780
Cutting speed [m/s]	4,66
Immersion depth [mm]	1

Table 3. Tool microgeometry brushed and unprepared.

Microgeometry	Δr [µm]	Sα [µm]	Sγ [µm]	K [-]
After brushing	21.0	26,.9	62.1	2.3
Unprepared	3.5	8.0	8.3	1.03

2.3. Measuring systems

In Hammering Turning the synchronized displacement of the tool in two axes is important. The exact displacement of the tool is however not known, since the piezo actuators operate in an open-loop mode and therefore the displacement, which is influenced by process forces and elasticity, is not known. For the displacement measurement, three capacitive distance sensors of the type Micro-Epsilon S601-0.2 were integrated into the tool system. The sensors are assigned to the three spatial directions. These are the movement of the tool in x-direction, the direction of the hammering movement and the movement in y-direction, the direction of oscillation and cutting direction. The third sensor monitors any process-related displacements in the z-direction, the feed direction of the turning process. The three sensors can thus measure translational displacements of the tool, but not rotational ones, although these should be minimal due to the kinematics of the solid-state joint. In order to be able to measure the spatial displacements of the cutting insert as precisely as possible, the measurement was carried out directly behind the cutting insert at the solid-state joint. The process forces were measured on the tool side using a Kistler type Z 3393 multicomponent dynamometer with a sampling frequency of *4.5 kHz*.

2.4. Microscopic analysis of the surfaces

To characterize and analyze the resulting surface topographies, a µsurf confocal microscope from NanoFocus was used. Using an Olympus objective with 20x magnification, *800 µm* by *800 µm* areas of the sample surface were mapped. For the evaluation of the topography, a shape removal of the curved surface of the cylindrical samples was carried out first. From these corrected surfaces, the height and spatial parameters of the surface were extracted according to ISO 25178.

3. Results and discussion

3.1. Process forces

During the measurement of the process forces on the tool side, there is a strong superposition of the effective process forces applied to the workpiece with mass inertia forces due to the vibration excitation. Figure 2 shows an example of the periodic force signal curve for the three spatial directions, for a feed rate of *0.01 mm/rev*. The signal is periodically averaged over *1000* periods, the scattering width of the signal is shown with a background color. The signal clearly shows the positive and negative force pulse in the x-direction of the hammering stroke, which is caused by the acceleration of the tool. The force signal in y-direction, the cutting direction, is superimposed by strong variations, but in the area of the hammering pulse a drop of the force can be seen, this is caused by the reduced cutting speed by the superimposed sinusoidal oscillation, also a drop due to the retraction movement of the tool cannot be excluded. Since there are no forced oscillations in the z-direction, the feed direction, and the cutting depth and feed are relatively small for turning processes, no significant forces are observed here. Figure 3 shows the maximum and minimum values of the measured forces for different feed rates and cutting edge microgeometries. With regard to the maximum x-forces, no pronounced change can be observed over the feed rate and microgeometry, fluctuations seem to be rather unsystematic due to process deviations. For the minimum values of the force, there seems to be a tendency, that the more rounded cutting edge shows slightly smaller values. However, when considering the minimum y-forces in the cutting direction, there is a tendency for the influence of the feed rate to lead to a decrease in the maxima and minima.

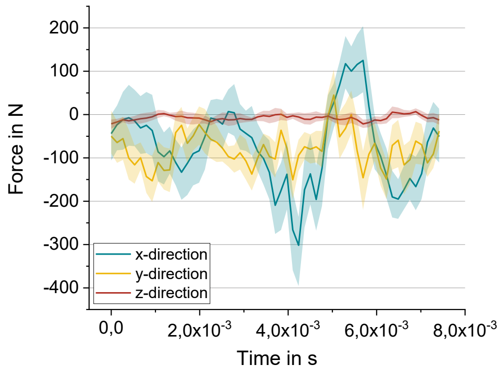

Figure 2: Periodic force-signal curve for the three spatial directions.

Since the maximum and minimum values cannot be clearly separated between forces from inertia and process forces, the averaged force values must be considered. Since the inertia forces always have both a negative and a positive component, which neutralize each other in their integrals, these also disappear for the mean value. The mean value therefore only contains forces that are applied to the mass system of the tool system from externally, whereby these are the effective averaged process forces. Figure 4 shows these calculated averaged forces. For the x-direction, which corresponds to the hammering direction or the passive force, the result, which is to be expected from an external turning process, is clearly visible. Increasing feed also leads to an increase in the magnitude of the averaged forces. This can be explained by the increased contact area between the toolpath and the workpiece due to the greater distance between the individual toolpaths.

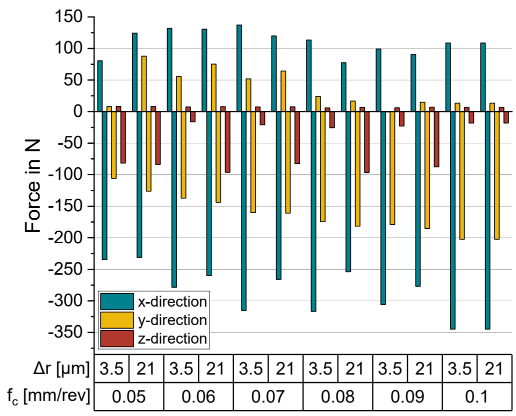

Figure 3: Maximum and minimum values of the measured forces.

The same results for the forces in the cutting direction. As expected, the increased feed rate due to the increased cutting area also leads to higher forces in this case. For the averaged forces in the feed direction, z-direction, there is an interesting influence of the cutting edge microgeometry. Almost independently of the feed, similar forces are measured, although these are significantly greater for the more rounded cutting edge. The experiments with a feed rate of *0.05* and *0.1 mm/rev* are an exception.

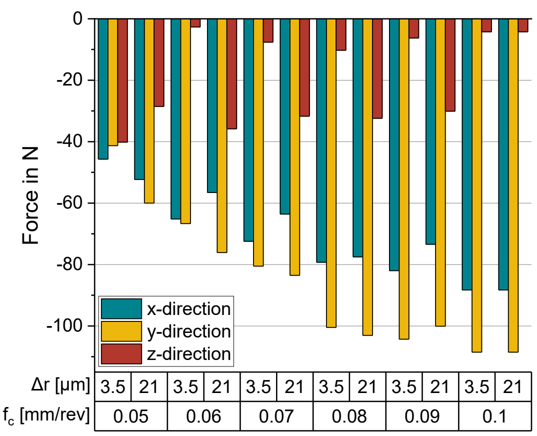

Figure 4: Calculated averaged forces.

3.2. Measurement of tool displacement

In addition to the force measurement, the effective displacements in the cutting direction and hammering direction are decisive for the characterization of the process. Figure 5 shows exemplarily the measured motion trace during the Hammering Turning of the tool with the capacitive displacement measurement system. In the x-y color plot diagram all measured values over *1000* oscillation periods are shown. The full line represents the average value. It can be clearly seen that the deviation band is very narrow with only a few micrometers. The dashed line shows the trajectory of the tool movement without a tool-workpiece contact. It is noticeable that especially the displacement in the x-direction is strongly influenced and the hammering stroke is also deflected in the y-direction. This can be explained by the fact that the maximum deflection of the piezo actuator is not reached due to the workpiece contact and the resulting forces. Also, the remaining relative velocity between the tool and the workpiece, which does not disappear completely because the nominal displacement of $\pm 10\ \mu m$ in the y-direction is not reached, causes a shift of the peak.

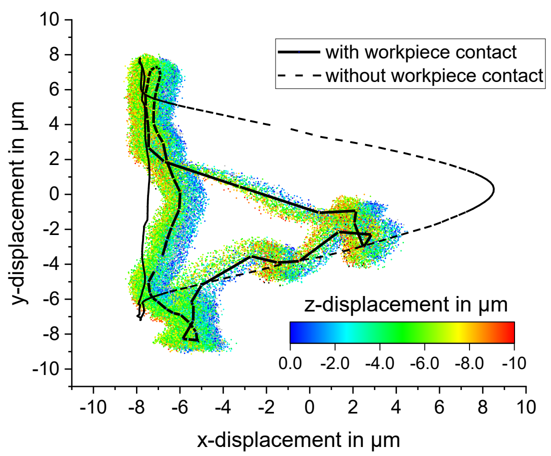

Figure 5: Motion trace during hammering turning.

The absolute experimental displacements (peak to peak) for the spatial directions and tool microgemeotries are shown in Figure 6 for different feed rates with workpiece contact. It is particularly interesting to note that the height of the hammer stroke, x-direction, is not changed by the feed rate. This is not to be expected, since the larger feed rate also results in a larger contact area and, as shown in Figure 3, a higher force. This speaks for a very precise tooling system, which ensures a stable displacement of the piezo actuators independent of the process parameters. Also, small differences in the displacement are seen depending on the microgeometries of the tools. Sharp-edged tools seem to lead to slightly smaller displacements, at least for the medium feed rate range. However, this may also be related to the slightly larger forces with sharp-edged tools, as shown in Figure 3. For the vibration excitation in the cutting direction, y-direction, the same tendency can be observed. The feed rate has no relevant influence on the displacement, even in this direction the displacement of the tool seems to be less reduced by the workpiece contact. This can be explained by the lower forces in this direction. Here the tool microgemetry has nearly no influence, a minimal decrease can be seen with the rounded tool. In the feed direction, there is no active displacement by piezo actuators in the process, but a displacement can be measured here. This is caused by unintentional vibrations and the relatively low rigidity of the aluminum solid-state joint in the z-direction, which must allow the tool to move in the x and y-directions. Since this displacement is in the range of a few micrometers, it is not important for the process and does not need to be considered. It can be concluded that the piezo system operates stably and with high repeatability in the investigated range.

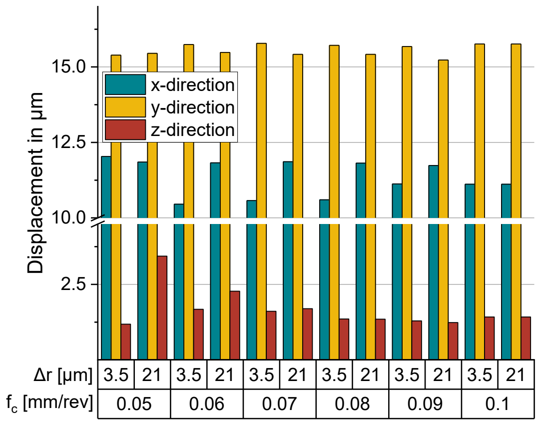

Figure 6: Total displacements (peak to peak) with workepiece contact for the spatial directions.

3.3. Optical investigation of the topography

The focus of this investigation is to identify the influence of tool microgeometry and feed rate in the Hammering Turning process on the resulting microtextured topography. Figure 7 shows the confocal microscope images of the surfaces for the different cutting edge microgeomtries and feeds. There is a clear optical difference between the microgeometries. The tool with a larger rounding creates a topography with flat dimple-shaped indentations, which are separated from each other by the feed marks. The distance of the indentations in the surface in the cutting direction is $63\ \mu m$, due to the cutting speed and frequency of the process, regardless of the feed rate. For the sharp-edged cutting tool, the indentations look different, they are comma-shaped and do not have an orthogonal orientation

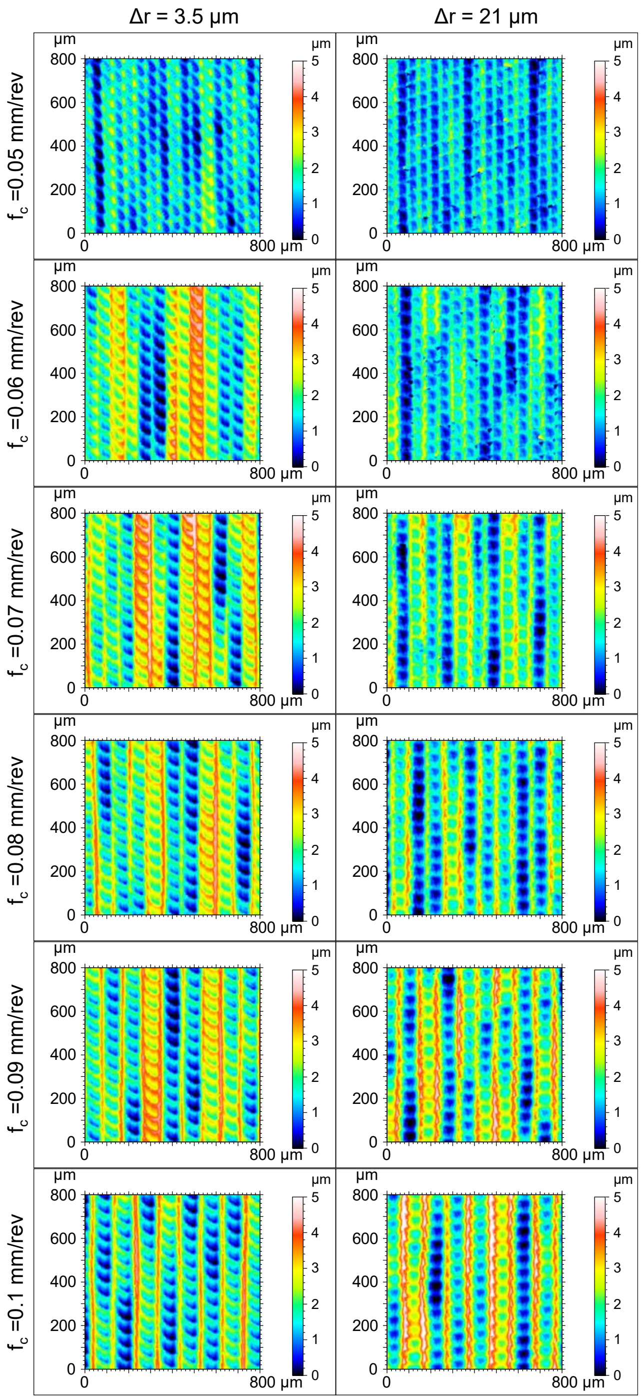

Figure 7: Confocal microscopy images of the surfaces.

to the cutting direction, as would be expected from the angle of attack of the tool. In this case, the microgeometry along the cutting edge does not seem to be exactly uniform, so that, in simplified view, the tool does not contact the surface in a line of contact and deforms it, giving the indentation a comma-shaped morphology. The feed has little influence on the basic pattern of the microtexture in contrast to the microgeomtry of the tool, it only increases the distance between the tool paths and the feed marks become more pronounced. An exception is the surface with a feed rate of *0.05 mm/rev* for the sharp-edged tool. The indentations overlap so much that the usual morphology of the topography of indentations in a surface tends to a topography where peaks emerge from a surface.

So far, this is only an optical subjective analysis, for the evaluation of the microtextured surfaces and for the comparison with other surfaces a calculation of surface parameters has to be done. The figure also shows deviations in the height of the single tool paths, which can possibly be attributed to the low rigidity of the tool. As the solid-state joint must allow movement in two axes, this is a compromise between rigidity and flexibility in two axes, which can lead to such inhomogeneities in the process. Figure 8 shows the measured surface parameters Sa and Sz, the evaluation of these rather simple parameters shows that the Sa value increases with the feed rate, as expected. For the prepared tool, the values are increasing with the feed, for the sharp-edged tool, variations can be seen. It also shows that for the sharp-edged tool the values are almost always higher than for the rounded tool. The same can be noticed for the Sz value. The topography obtained with the rounded tool thus seems to have less high peaks on the surface. This can possibly be caused by the larger contact area of the tool, which leads to a slight smoothing of the surface. Also, the topography of the tool itself may have an influence here, as it behaves like a die and transfers its own topography to the workpiece. In the case of the rounded tool, a smoother surface is achieved by preparation by brushing.

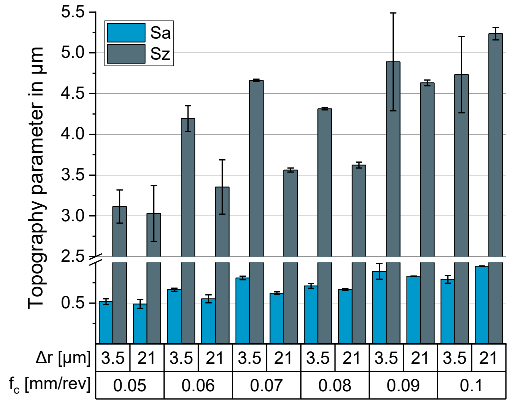

Figure 8: Measured surface parameters Sa and Sz.

For better analysis of the topography, it is helpful to use the Abbott-Firestone curves and their parameters. Figure 9 shows the calculated Sk, Spk and Svk parameters. The Sk parameter, the core height, increases with increasing feed rate, which is to be expected since the total height of the topography also increases in the form of the Sa and Sz values. This can be explained by the increasing influence of the kinematic roughness caused by the feed rate. The value varies and partially deviates upwards for the sharp cutting edge geometry and also downwards for a feed rate of *0.1 mm/rev*. A systematic difference between the microgeometries cannot be observed. When considering the reduced peak height Spk, an interesting behavior is seen for the feed rate, up to a rate of *0.08 mm/rev* there is hardly any increase, but above this rate there is a significant increase. This may be related to the width of a tool indentation in the feed direction, above this value the influence of the kinematic roughness dominates, below that that of the texturing. This clear limit of the feed cannot be found in the reduced valley height Svk. However, in this parameter the influence of the cutting edge microgeometry, already seen in

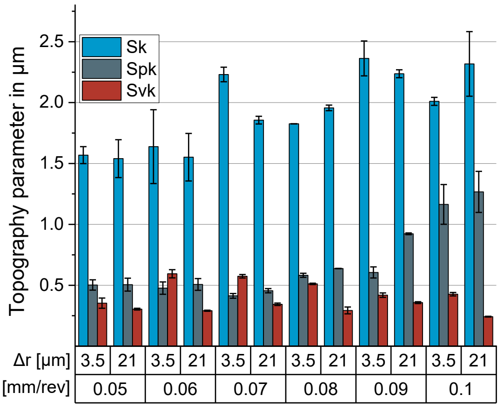

Figure 9: Calculated Sk, Spk and Svk values from Abbott-Firestone curves.

the optical evaluation, can be found. Especially at low feed for the rounded tool, on the other hand, the feed rate has no visible influence on the value. An exception represents here again the smallest feed rate with *0.05 mm/rev*. In this case, probably due to the large overlap of the tool indentation in relation to the tool path distance, other mechanism seem to have an effect.

For many tribological functional surfaces, low Spk values and larger Svk values are aimed for. This describes a plateau-like surface with deep grooves. The oil retention volume can be determined directly from the Svk value. It is possible to quantify how deep the area is in which a liquid applied to the surface collects. In this way, it is possible to improve the lubrication properties.

For Hammering Turning it can be concluded that for such tribologically loaded surfaces a feed rate of *0.06 -0.07 mm/rev* should be the most suitable.

4. Conclusion and outlook

In this work, the influence of the cutting edge micro-geometry and the feed rate on the Hammering Turning was investigated. For this purpose, different variables in the process were measured and analyzed, these were the process forces and displacements of the tool, as well as the resulting microtextured surfaces. The following key findings were obtained:

- The process forces show a strong superposition with inertia forces due to the vibration excitation, which is periodic and very repetitive with low deviation.
- The average forces in the cutting direction and normal to the surface increase with increasing feed rate, but the force in feed direction itself is hardly affected. Cutting edges with a greater rounding lead to greater forces.
- The tool displacements measured in the process are not affected by the feed rate, so the piezo tool system works very reliably.
- Cutting edge microgeometry has a significant influence on the topography of the microtexture.
- Sa and Sz values show variations, with sharp-edged tools having higher values.
- Reduced valley depth Svk shows differences between microgeometries, with sharp-edged tools producing deeper valleys.
- The reduced peak height Spk can be influenced by the setting of the feed rate f_c.

These findings are crucial for characterizing Hammering Turning and optimizing tribological surface properties. In further investigations, tribological tests on cylinder-on-disc tribometers will be carried out to investigate the wear behavior and friction coefficients of this microtextured surface. This finding is the basis for an inverse approach for Hammering Turning, which allows the friction coefficient of such surfaces to be adjusted based on the knowledge of the tribological behavior of such microtextures. As the microtextures are incorporated by plastic deformation of the surface in this process, it is to be expected that compressive residual stresses and hardness will increase. Which results in increased wear resistance. This should be investigated in future studies. In the work of Liu et al. it was reported that such textures can have an influence on the tribological behavior and can reduce the friction coefficient [13]. But these can wear out very quickly, reducing their effectiveness. Although the study used brass rather than steel, the mechanisms may be similar. However, these micro-textures are formed by cutting alone, there is no superimposed oscillation in the cutting direction, so the change in the surface layer due to plastic deformation is minimal and no mechanical surface treatment takes place. Another aspect of textured surfaces is their influence on fatigue strength, as topography, hardness and residual stresses have a major influence. Investigations with rotary bending tests are also planned in order to show the difference to turned surfaces.

Acknowledgements

The authors thank the German Research Foundation for funding this study as part of the research project ZA 785/4-2.

References

[1] Brehl, D.E., Dow, T.A., 2008. Review of vibration-assisted machining *32*, p. 153.
[2] Skelton, R.C., 1968. Turning with an oscillating tool *8*, p. 239.
[3] Zheng, L., Chen, W., Huo, D., 2020. Review of vibration devices for vibration-assisted machining *108*, p. 1631.
[4] Liu, X., Wu, D., Zhang, J., 2018. Fabrication of micro-textured surface using feed-direction ultrasonic vibration-assisted turning *97*, p. 3849.
[5] Liu, X., Wu, D., Zhang, J., Hu, X. *et al.*, 2019. Analysis of surface texturing in radial ultrasonic vibration-assisted turning *267*, p. 186.
[6] Schubert, A., Nestler, A., Pinternagel, S., Zeidler, H., 2011. Influence of ultrasonic vibration assistance on the surface integrity in turning of the aluminium alloy AA2017 *42*, p. 658.
[7] Zhang, R., Steinert, P., Schubert, A., 2014. Microstructuring of Surfaces by Two-stage Vibration-assisted Turning *14*, p. 136.
[8] Kumar, M.N., Subbu, S.K., Krishna, P.V., Venugopal, A., 2014. Vibration Assisted Conventional and Advanced Machining: A Review *97*, p. 1577.
[9] Fuchs, M., Habersohn, C., Kalkan, Y., Lechner, C. *et al.*, 2015. Metrological investigation of an actuator device for vibration assisted turning *43*, p. 119.
[10] Schwalm, J., Mann, F., Gerstenmeyer, M., Zanger, F. *et al.*, 2022. Main time-parallel mechanical surface treatment and surface texturing during machining *108*, p. 240.
[11] Schwalm, J., Mann, F., González, G., Zanger, F. *et al.*, 2023. Finite Element Simulation of the process combination Hammering Turning *117*, p. 110.
[12] Denkena, B., Leon, L. de, Bassett, E., Rehe, M., 2010. Cutting Edge Preparation by Means of Abrasive Brushing *438*, p. 1.
[13] Liu, X., Zhang, J., Li, L., 2021. Surface Integrity and Friction Performance of Brass H62 Textured by One-Dimensional Ultrasonic Vibration-Assisted Turning. Micromachines (Basel) *12*.